Miniaturized 3-D Solenoid-Type Micro-Heaters in Coordination With 3-D Microfluidics

Hao Bian, Chao Shan, Feng Chen, Qing Yang, Yanyang Li, and Qichao Li

***Abstract*— We fabricate and characterize a prototype on-chip 3-D micro-heater inside a fused silica chip, which is coordinated with a microfluidic channel. By means of enhanced femtosecond laser wet etching followed by a micro-mold injection process of a liquid metal, the solenoid-type metallic micro-heater, with a size of $\pi \times 100^2 \times 1120\ \mu m^3$, was fabricated twining outward a linear microfluidic channel. The micro-heater exhibits excellent performances, such as precisely current-temperature controllability (temperature range from 0°C to 130°C), rapid heating/cooling process (up to 16 °C/s at the beginning of the heating process and 15.8 °C/s at the beginning of cooling process), and uniform temperature distribution. This work not only provides a high-quality micro-heater for biological or chemical applications, which requires rigid temperature control capabilities, but also proposes a practical route to the fabrication of comprehensive truly-3-D lab-on-a-chip devices and microelectromechanical systems. [2016-0215]**

***Index Terms*— Laser machining, micro-heater, micro-channels, 3-D microfluidics.**

I. Introduction

During the past decade, lab-on-a-chip (LOC) is well accepted to be a paradigm-shift technology in many fields such as life science, medicine, chemistry and environmental science [1]. In particular, microfluidics, one of the most important components in the LOC devices, has been intensively studied [2], [3]. Several approaches such as soft lithography, embossing and micro-machining were adopted to fabricate the microfluidics [4]–[6]. Current advances in femtosecond laser three-dimensional (3D) manufacturing and 3D printing enable the fabrication of 3D microfluidics in both glass and polymer substrates, which significantly improve the integration level as well as the performances of the device [7]–[9]. For a functional 3D LOC device which integrates several laboratory functions, the electronical components need to be 3D for matching with the 3D microfluidics. However, fabrication of such a comprehensive 3D LOC device is still a grand challenge for most current manufacturing technologies.

The major barrier for developing comprehensive 3D LOC devices lies in the lack of practical methods to fabricate integrated 3D micro-electronics or micro-sensors which are coordinated with complex microfluidic channels with 3D geometries. The simple combination of the existing 2D micro-electronics with 3D microfluidics brings obvious problems. For example, planar micro-heaters fabricated by the deposition and lift-off processes [10]–[12] could not create uniform temperature distribution throughout microchannel in 3D geometry, still weaken the precise control of the temperature. In some LOC applications such as microthrusters, electrophysiology and polymerase chain reactions [13], [14], which require strict control of the local temperatures, 2D micro-heaters have severely retarded the usage of 3D microfluidics whose performances are proved to be far beyond the planar microfluidics. To conquer this barrier, novel fabrication approaches are needed for the simultaneous generation of arbitrary 3D microelectronics which are coordinated with the 3D microfluidics. Some works utilized a microchannel filled with liquid-metal as an electrical heater in a microfluidic chip [15]–[17]. As most of the microchannels were fabricated by a soft lithography process which still results in a plane thermal source, the idea of micro-mold injection of liquid metal gives us a lot of inspiration.

In this paper, we propose an approach to the fabrication of integrated 3D micro-electronics which are coordinated with 3D microfluidics by an enhanced femtosecond laser wet etching (FLWE) followed by a micro-mold injection process [18]. As a demonstration, we fabricate a prototype LOC device which combines a 3D solenoid-type metallic micro-heater rolled outward a microfluidic channel in fused silica chip. The heating properties, including the current-temperature curve, maximum temperature, temperature evolution and the temperature distribution were measured by an infrared imager. The results demonstrate the rapid heating process, short responding time, precise temperature control and uniform temperature distributions of our device. Because of perfect alignment between the heating source, solenoid-type micro-heater, and the microfluidics, the temperature of the liquid samples in the microfluidics can be uniformly and precisely controlled, which is important for many applications such as polymerase chain reactions. The advantage of our technology lies in the freeform manufacturing of arbitrary 3D micro-molds and microfluidics simultaneously in the same substrates. By the injection of different materials, the configuration of 3D microfluidics, various electronics and sensors

Manuscript received September 2, 2016; revised February 20, 2017; accepted February 25, 2017. Date of publication March 20, 2017; date of current version May 31, 2017. This work was supported in part by the National Science Foundation of China under Grant 61475124, Grant 61275008, Grant 51335008, and Grant 61405154; in part by the Special-Funded Program on National Key Scientific Instruments and Equipment Development of China under Grant 2012YQ12004706; and in part by the China Post-Doctoral Science Foundation under Grant 2014M562414. Subject Editor A. Luque. *(Corresponding authors: Feng Chen; Qing Yang.)*

The authors are with the State Key Laboratory for Manufacturing System Engineering and the Key Laboratory of Photonics Technology for Information of Shaanxi Province, School of Electronics and Information Engineering, Xi'an Jiaotong University, Xi'an 710049, China (e-mail: chenfeng@mail.xjtu.edu.cn).

Color versions of one or more of the figures in this paper are available online at http://ieeexplore.ieee.org.

Digital Object Identifier 10.1109/JMEMS.2017.2676003

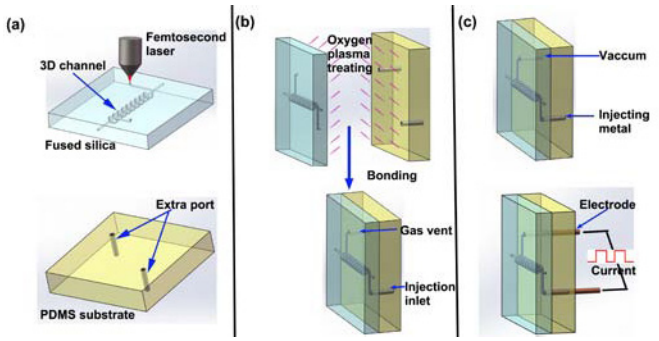

Fig. 1. Schematic illustration of the fabrication process of micro-heater. (a) Formation of 3D microchannels by femtosecond laser wet etch technology (upper image) and the PDMS substrate with two extra ports (lower image). (b) Bonding of the fused silica and the PDMS substrate. (c) Micro-mold injection of the liquid metal alloy (upper image) and assembly of electrodes to form the final device (lower image).

can be achieved without any other complicated, time-/cost-consuming alignment and packaging processes, which open up a new direction for practical manufacturing of comprehensive 3D LOC devices.

II. Method & Experimental

The fabrication process of the micro-heater involves our enhanced femtosecond laser wet etching technology [18], followed by a liquid metal micro-injection process. The process is divided into three steps, as illustrated in Fig. 1.

A. Fabrication of 3D Microchannels Inside Glass Substrate (Fig. 1(a))

First of all, a spiral-shaped microchannel is fabricated inside a fused silica chip by the enhanced femtosecond laser wet etching process, which can be served as a micro-mold for the solenoid-type micro-heater. The fabrication process is achieved by a femtosecond laser micromachining system which comprises a femtosecond laser source (wavelength: 800 nm, pulse duration time: 50 fs, repetition rate: 1 kHz), a computer programmable x-y-z stage, a microscope objective lens with numerical aperture (N.A.) of 0.9 and a CCD monitoring camera [19]. A fused silica chip ($10\times10\times0.8$ mm^3, six sides polished) is fixed on the stage, and direct writing of the spiral pattern is accomplished by translating the sample in a pre-designed path. The laser power is 5 mW, and the scanning speed is 10μm/s. To maximize the selectivity of the wet etching, we use the circularly polarized laser beam which is obtained by a $\lambda/4$ wave plate [18], [19]. After the laser direct writing, the sample is immersed in an ultrasound assisted hydrofluoric (HF) acid (10%) chamber for the wet etching. For the hollow spiral channel with a dimension of 35 μm, the etching time is about 1 hour. Simultaneously, straight microfluidic channel along the axis of solenoid micro-heater is fabricated by a similar approach. The inlet and outlet of the microfluidic channel are located on the sidewalls of the chip, while the injection ports of the micro-heater mold are on the upper surface which will be bonded with a polydimethylsiloxane (PDMS) sheet.

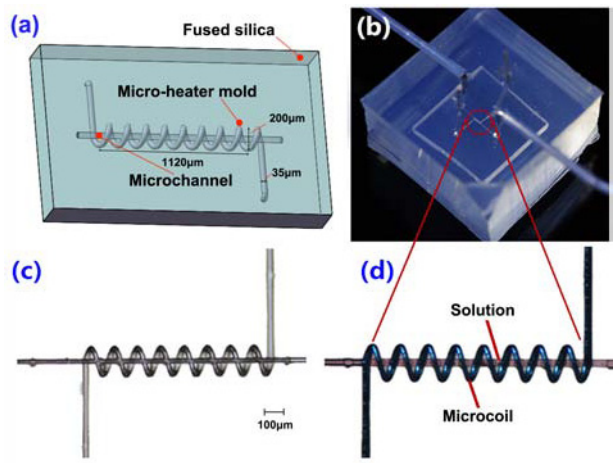

Fig. 2. (a) Schematic illustration of micro-heater molding; (b) micro-heater chip; (c) micro-heater before metal injection; (d) micro-heater after metal injection.

B. Bonding of PDMS Sheet on the Fused Silica Chip (Fig. 1(b))

To inject the liquid metal into the narrow 3D microchannels without bubbles, the injection port of the micro-heater mold should be tightly latched onto the injection tube. As shown in Fig. 1(b), two corresponding via-holes are punched on the PDMS sheet, and one of them latched the tube for the metal injection while the other is served as the gas venting port. Before the bonding process, the fused silica chip and the PDMS sheet were cleaned twice in the ethanol ultrasonic bath and dried by the nitrogen flow. The bonding surfaces of the fused silica and PDMS are then treated by the oxygen plasma for 60 seconds. During the bonding process, the punched via-holes on the PDMS are carefully aligned with the ports of the micro-mold before the two pieces are permanently connected with each other.

C. Micro-Mold Injection of Liquid Metal (Fig. 1(c))

To generate the metallic solenoid-type micro-heater, the liquid metal (an alloy comprised of bismuth, stannum, lead, and indium, with a melting point of 95°C, Suzhou chuan MAO metal materials co., LTD, China) is injected into the spiral channel to form a metal coil, and electrodes are inserted into the PDMS via-holes and contact with the metal coil. A PTFE (polytetrafluoroethylene, the temperature tolerance: 260°C) tube was used to guide the liquid metal which is melted at 120°C in a heating chamber. During the injection process, negative pressure was applied to the gas venting port by a vacuum pump, ensuring the microchannel is filled with the liquid metal without bubbles. After the liquid metal cools down to the room temperature, we examined the conductance of the micro-heater by an ohmmeter and get a resistance of 1-2 ohm.

III. Results and Discussion

The schematic illustration of the micro-heater and the microfluidic channel is shown in Fig. 2(a). Fig. 2(b) shows

the optical micrograph of the miniaturized micro-heater with two extra ports which we demonstrated in the manuscript. The mold of the micro-heater is a spiral channel with a diameter of 200 μm. Its 8 windings twine around the straight microfluidic channel with diameter of 35±2 μm. As demonstrated in Fig. 2(c), our enhanced femtosecond laser wet etch technology [18], which combines the utilize of circular-polarized laser beam, extra access ports and power compensation strategies, can fabricate complex 3D microchannel with extremely high aspect-ratio, uniform diameter and smooth inner surface. In particular, the circular-polarized femtosecond laser results in the random nano structures [19], extra access ports reduce the wet etching time, power compensation benefits the uniformity of the microchannel. These strategies ensure the large aspect-ratio and uniform 3D microchannel which is critical to obtain identical resistance along the solenoid-type micro-heater. Fig. 2(d) shows the curved metal wire with diameter of about 35±2 μm. The cross-sectional area of the micro-heater is $\pi \times 100^2 \mu m^2$, and the length is 1120 μm, which meets the demands of miniaturization and integration of the contemporary biochips. Due to the negative pressure added on gas venting ports, bubbles and discontinue of the metal wire cannot be observed under the microscope. The microfluidic channel is fabricated in the center of the solenoid micro-heater, and liquid samples could be heated uniformly when they flow through the microchannel. For the technology proposed in this work, we could not see any technical barriers to fabricate more complex 3D microfluidics with twined solenoid micro-heaters [20], [21].

We tested the heating process by loading different input electrical current. The temperature of the micro-heater (in the plane perpendicular to the axial direction of the spiral coils) is obtained by an infrared thermal imager (SC7300M, FLIR System AB). The IR thermal imager is a well-established measurement technique to measure, nonintrusively, local temperatures in the range of tens to hundreds of micrometers. And special calibration process is needed to get an actual temperature [22]. In our experiment, a simple calibration process was adopted via the software by measuring a metal material inside the glass with a known temperature. And the current-temperature curves are plotted in Fig. 3(a). For the current of 0.25 A, the stable temperature is about 25 °C, close to ambient temperature. When the current increases to 1.04 A, the temperature reaches to 104 °C within 20 s, about 80% to the maximum temperature of 120 °C after 200 s, demonstrating a rapid heating process which is an important factor for the micro-heaters. However, it will need a relatively long time to get the maximum temperature. So in practical applications, high current could be used in heating period in which the sample is heated to high temperature in a short time instead of waiting for a long time to get the maximum temperature, and then low current could be applied for the heat preservation. It indicates that the maximum temperature can be precisely controlled to the current loaded on the micro-heater. According to Joule's law, $Q = I^2RT$ (where Q, energy; I, current; R, resistance; and T, time), a similar quadratic relationship exists between heat and current. The relationship between the maximum temperature and the loaded current is

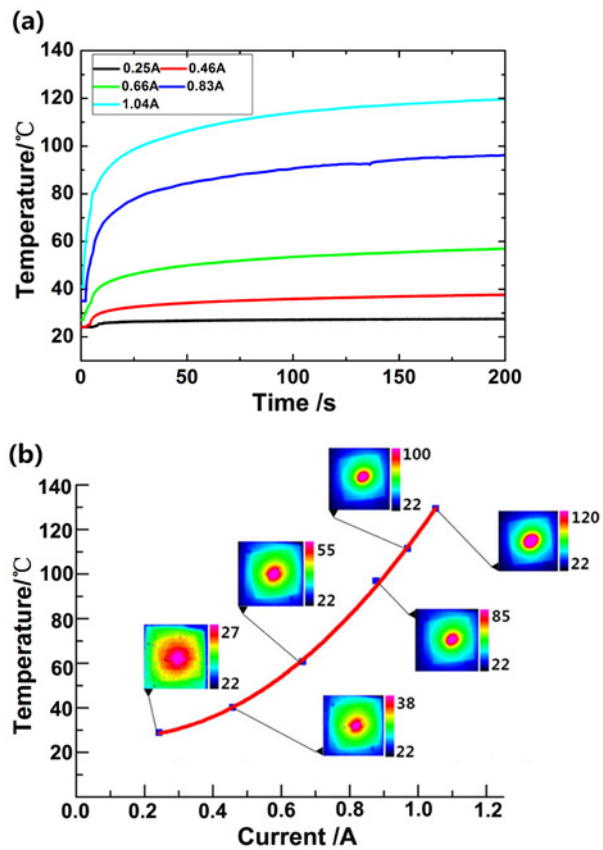

Fig. 3. (a) Heating properties of the micro-heater at different electric currents. (b) Maximum temperature and corresponding infrared thermal images at different electric currents. The each image size of insert temperature distribution images is about 10 mm×10 mm. Please note different values of the temperature bars.

plotted in Fig. 3(b). The temperature distribution images at different current are also shown in the figure. It should be mentioned that R, resistance, is also related to the temperature of the metal [15]. And when we load the current bigger than 1.1 A, the liquid metal will change from the solid state to the liquid state and the corresponding resistance will be changed nonlinearly. Even worse the metallic microchannel will get disconnected. So we generally load the current under the 1.04 A.

The infrared thermal images show detailed information of the thermal distribution, which can be used for a straightforward observation of the temperature evolutions in the microfluidic channel (located in the middle of the images) during and after the heating period. Fig. 4(a) and (b) show the evolution of temperature distribution and the heating rate at the current of 1.04 A, respectively. The heating rate of the microfluidic rises up to 16 °C/s at the very beginning when the current loaded on the micro-heater, indicating the rapid response of heating process. The temperature in the microfluidic channel reaches to the 80% maximum of 130 °C at 20 s. Afterward, it rises slowly while the thermal expands and heats the ambient region. Interestingly, although the maximum temperature in the microchannel and micro-heater is already higher than the melting point of the liquid metal, the device is still functioning

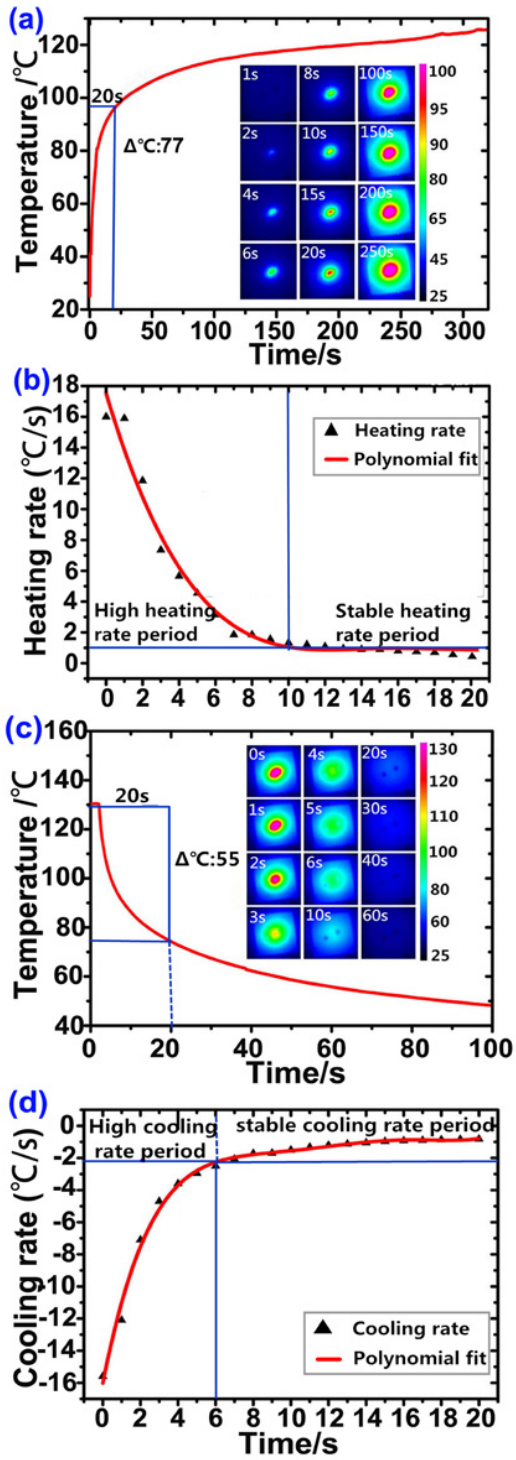

Fig. 4. (a) The heating property at the highest electric current of 1.04 A and the infrared thermal image figures at different time. The each image size of insert temperature distribution images is about 10 mm×10 mm. (b) The heating rate in beginning 20 s of heating period. (c) The cooling process after electric current of 1.04 A is off and the infrared thermal images at different time. The each image size of insert temperature distribution images is about 10 mm×10 mm. (d) The cooling rate in beginning 20s of cooling period. Please note the different bars of (a), (c) and (b), (d).

because the melted metal can be limited inside the mold and keeps heating the surroundings. It provides a simple method to squeeze the capability of micro-heaters beyond the limit of resistance of the material. Fig. 4(b) directly indicates the fast

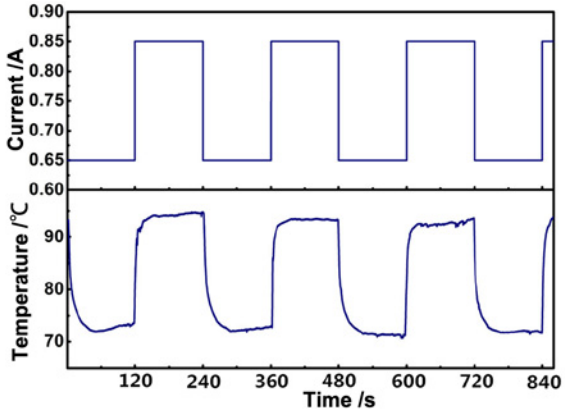

Fig. 5. Periodic variation of temperature with the periodic square electric current.

current response of the heating process. The highest heating rate can be obtained once the current is loaded, and relative high heating rate can last about 10 s. The cooling of the micro-heater is also impressive, as demonstrated in Fig. 4(c) and (d). The highest cooling rate can be up to 15.8 °C/s, at very beginning when the power is off, and drops quickly in the subsequent 6 s. Such a non-linear cooling process could be related to the phase transition of the liquid metal. The temperature declines sharply during the re-solidification period of the metal, and the speed slows down when the temperature is just lower than the melting point of metal alloy. What's more, the cooling process presented in Fig. 4 is slower compared to the heating process as the glass substrate is a poor conductor of heat which will benefit the micro-heater with a stable temperature. There are also some facial processes we can adopt to obtain a fast cooling process, like water-cooling or compressed air flowing.

Such rapid response of heating and cooling processes provides a flexible control of the temperature inside the microfluidic channel. To demonstrate the controllability of our device, pulsed current is applied. The current and corresponding temperature is shown in Fig. 5. The high/low current pulses of 0.85A/0.65A with period of 120 s induce the maximum/minimum temperature of 94°C/71°C, and almost no delay of temperature responses can be observed. This property allows us to develop LOC devices with programmable accurate temperature control function by introducing a temperature feedback system. A high current can be applied to heat the sample to the interesting temperature within a few second, and feedback signal switches current to low level for preserving the temperature. It should be mentioned that for the same electrical current, the temperature we obtained in Fig. 5 is higher than in Fig. 3. It is because that there is some heat preserved inside the micro-heater as the glass substrate is a poor conductor of heat.

The uniformity of the temperature distribution produced by the micro-heater is also investigated. Under the current of 1.04 A, the temperature distribution image is captured after 60 seconds of heating (insert of Fig. 6). The temperature is measured along the two diagonal (a-a', b-b') directions and plotted in Fig. 6. We can easily observe the "flat-top" in the middle of two curves, which shows the identical temperature

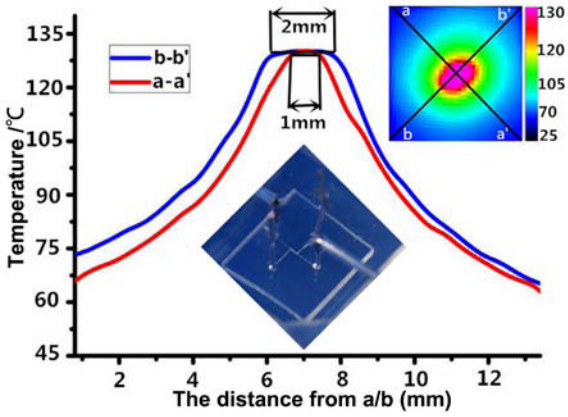

Fig. 6. Temperature distributions along the diagonal directions of the infrared thermal image figure. The each image size of insert temperature distribution images is about 10 mm×10 mm.

in the middle of the micro-heater. The uniform temperature (the width of "flat-top") covers a large area of 1 mm by 2 mm (about 1 mm in a-a' direction, and 2 mm in b-b' direction). It means, in the microfluidic channel with diameter of tens of micrometers (locate in the middle of the insert graph in Fig. 6), the temperature is highly uniform. Such uniform temperature distribution cannot be obtained in the microfluidic channel combined with a flat micro-heater. It is common to obtain gradient temperature distribution if the heat source is mounted on one side of the microfluidic channel.

IV. Conclusions

In this paper, we presented a prototype on-chip 3D micro-heater incubated inside fused silica utilizing an enhanced femtosecond laser wet etching followed by micro-mold injection process. The spiral microchannel was fabricated inside fused silica chip as the mold, and solenoid-type micro-heater was generated by injecting the liquid metal into the mold. The experimental results demonstrated the capabilities of the device, including precise control of the temperature by the current, rapid heating and cooling process and uniform distribution of the temperature inside the microfluidic channel, which are important for applications requiring precisely localized temperature control, such as polymerase chain reactions. Our technology could be used to fabricate various integrated micro-electronics, micro-sensors and microfluidics in a single process by applying different injection materials. This work paves a new avenue to develop next-generation 3D LOC devices or MEMS which need to integrate and coordinate multiple complicated components into a single chip.

References

[1] R. Daw and J. Finkelstein, "Lab on a chip," *Nature*, vol. 442, no. 7101, p. 367, Jul. 2006.

[2] G. M. Whitesides, "The origins and the future of microfluidics," *Nature*, vol. 442, no. 27, pp. 368–373, Jul. 2006.

[3] S. Haeberle and R. Zengerle, "Microfluidic platforms for lab-on-a-chip applications," *Lab Chip*, vol. 7, no. 9, pp. 1094–1110, Apr. 2007.

[4] M. E. Wilson *et al.*, "Fabrication of circular microfluidic channels by combining mechanical micromilling and soft lithography," *Lab Chip*, vol. 11, no. 8, pp. 1550–1555, Mar. 2011.

[5] N. S. G. K. Devaraju and M. A. Unger, "Pressure driven digital logic in PDMS based microfluidic devices fabricated by multilayer soft lithography," *Lab Chip*, vol. 12, no. 22, pp. 4809–4815, 2012.

[6] V. N. Goral, Y. Hsieh, O. N. Petzold, R. A. Faris, and P. K. Yuen, "Hot embossing of plastic microfluidic devices using poly(dimethylsiloxane) molds," *J. Micromech. Microeng.*, vol. 21, no. 1, pp. 017002-1–017002-8, Jan. 2011.

[7] R. Osellame, G. Cerullo, and R. Ramponi, "Femtosecond laser micromachining," in *Photonic and Microfluidic Devices in Transparent Materials*, vol. 123. New York, NY, USA: Springer, 2012.

[8] Y.-L. Zhang, Q.-D. Chen, H. Xia, and H.-B. Sun, "Designable 3D nanofabrication by femtosecond laser direct writing," *Nano Today*, vol. 5, pp. 435–448, Sep. 2010.

[9] C. M. B. Ho, H. N. Sum, K. H. H. Li, and Y. J. Yoon, "3D printed microfluidics for biological applications," *Lab Chip*, vol. 15, no. 18, pp. 3627–3637, Jul. 2015.

[10] H. R. Chen, C. Gau, B. T. Dai, and M. S. Tsai, "A monolithic fabrication process for a micro-flow heat transfer channel suspended over an air layer with arrays of micro-sensors and heaters," *Sens. Actuators A, Phys.*, vol. 108, nos. 1–3, pp. 81–85, Nov. 2003.

[11] A. Faraon and J. Vuckovic, "Local temperature control of photonic crystal devices via micron-scale electrical heaters," *Appl. Phys. Lett.*, vol. 95, no. 4, pp. 043102-1–043102-3, Jul. 2009.

[12] A. Scorzoni *et al.*, "Design and experimental characterization of thin film heaters on glass substrate for lab-on-chip applications," *Sens. Actuators A, Phys.*, vol. 229, pp. 203–210, Jun. 2015.

[13] J. Lee, K. Kim, and S. Kwon, "Design, fabrication, and testing of MEMS solid propellant thruster array chip on glass wafer," *Sens. Actuators A, Phys.*, vol. 157, no. 1, pp. 126–134, Jun. 2010.

[14] J. N. Yang *et al.*, "High sensitivity PCR assay in plastic micro reactors," *Lab Chip*, vol. 2, pp. 179–187, Nov. 2002.

[15] J. Je and J. Lee, "Design, fabrication, and characterization of liquid metal microheaters," *J. Microelectromech. Syst.*, vol. 23, no. 5, pp. 1156–1163, Oct. 2014.

[16] J. B. Wu, W. B. Cao, W. J. Wen, D. C. Chang, and P. Sheng, "Polydimethylsiloxane microfluidic chip with integrated microheater and thermal sensor," *Biomicrofluidics*, vol. 3, no. 1, pp. 012005-1–012005-7, Jan. 2009.

[17] M. Gao, L. Gui, and J. Liu, "Study of liquid-metal based heating method for temperature gradient focusing purpose," *J. Heat Transf.*, vol. 135, no. 9, p. 091402, Feb. 2013.

[18] S. He *et al.*, "Fabrication of three-dimensional helical microchannels with arbitrary length and uniform diameter inside fused silica," *Opt. Lett.*, vol. 37, no. 18, pp. 3825–3827, 2012.

[19] C. Hnatovsky, R. S. Taylor, E. Simova, V. R. Bhardwaj, D. M. Rayner, and P. B. Corkum, "Polarization-selective etching in femtosecond laser-assisted microfluidic channel fabrication in fused silica," *Opt. Lett.*, vol. 30, no. 14, pp. 1867–1869, 2005.

[20] F. Chen *et al.*, "Process for the fabrication of complex three-dimensional microcoils in fused silica," *Opt. Lett.*, vol. 38, no. 15, pp. 2911–2914, 2013.

[21] C. Shan *et al.*, "High-level integration of three-dimensional microcoils array in fused silica," *Opt. Lett.*, vol. 40, no. 17, pp. 4050–4053, 2015.

[22] J. M. Son, J. H. Lee, J. Kim, and Y. H. Cho, "Temperature distribution measurement of Au micro-heater in microfluidic channel using IR microscope," *Int. J. Precis. Eng. Manuf.*, vol. 16, no. 2, pp. 367–372, Feb. 2015.

Authors' photographs and biographies not available at the time of publication.